Adhatoda Vasica ameliorates cellular hypoxia dependent mitochondrial dysfunction in acute and severe asthmatic mice.

Atish Gheware[1,2,3,5], Lipsa Panda[4,5], Kritika Khanna[4,5], Vaibhav Jain[4,5], Naveen Kumar Bhatraju[4], Shakti Sagar[4,5], Manish Kumar[4], Vijay Pal Singh[4], Mitali Mukerji[1,2,3,5], Anurag Agrawal[4,5*] and Bhavana Prasher[1,2,3,5*]

1. Genomics and Molecular Medicine, Council of Scientific and Industrial Research -Institute of Genomics and Integrative Biology (CSIR-IGIB), Delhi, India.
2. CSIR's Ayurgenomics Unit–TRISUTRA (Translational Research and Innovative Science ThRoughAyurgenomics) CSIR-IGIB, Delhi, India.
3. Centre of excellence for Applied Development of Ayurveda, Prakriti and Genomics, CSIR- IGIB, Delhi, India.
4. Centre of excellence for Translational Research in Asthma & Lung disease, CSIR- IGIB, Delhi, India.
5. Academy of Scientific and Innovative Research (AcSIR), CSIR-IGIB, Delhi, India.

* bhavana.p@igib.res.in, a.agrawal@igib.in

Keywords

Severe asthma, steroid resistance, hypoxia, Ayurveda, *Adhatoda Vasica*.

Abstract

Severe asthma is chronic airway disease, exhibit poor response to conventional asthma therapies. Growing evidence suggests that elevated hypoxia increases the severity of asthmatic inflammation among patient and model systems. In this study, we elucidate the therapeutic effect and mechanistic basis of *Adhatoda Vasica* (AV) aqueous extract on acute allergic as well as severe asthma subtypes, at physiological, histopathological and molecular levels using mouse models. We observed, oral administration of AV extract not only attenuates the increased airway resistance and inflammation in acute allergic asthmatic mice but also alleviates the molecular signatures of steroid (dexamethasone) resistance like IL-17A, KC and HIF-1α (hypoxia inducible factor-1alpha) in severe asthmatic mice. The reversal of pathophysiological features after AV treatment is associated with inhibition of elevated HIF-1α levels by restoring the expression of its negative regulator-PHD2 (prolyl hydroxylase domain-2). This was further confirmed in acute and severe

asthma model developed by augmented hypoxic response. Further, AV treatment reverses cellular hypoxia- induced mitochondrial dysfunction in human bronchial epithelial cells - evident from bioenergetic profiles and morphological analysis of mitochondria. Involvement of hypoxia and mitochondrial dysfunction in asthma severity is being increasingly realised. Extract of AV although widely used in *Ayurveda* practice for the treatment of diverse respiratory ailments, including asthma, its molecular basis of action and effect on severe asthma subtype is still unclear. This study, demonstrates therapeutic mechanism of *Adhatoda Vasica* through hypoxia-induced mitochondrial dysfunction and highlights its potential in the treatment of severe steroid-resistant asthma.

Significance Statement

Severe asthma is a global health concern found to be unresponsive to current treatment modalities involving corticosteroids. Recent findings suggest that elevated hypoxia has a critical role in severity of asthma. Here, we report therapeutic treatment with aqueous extract of *Adhatoda Vasica* (AV), an ayurvedic medicine, is effective in attenuation of severe steroid-insensitive asthmatic features in mice. The observed anti-asthmatic effects of AV was through inhibition of hypoxic response, both *in vivo and in vitro*. AV also reverses mitochondrial dysfunction, a key consequence associated with hypoxia, and asthma. This study not only highlights the translational potential of AV for the treatment of severe asthma but also provides opportunities for its usage in other disease conditions where hypoxia is pertinent.

Introduction

Asthma is a complex and heterogeneous disease that involves recurrent, partially reversible bronchial obstruction. Airway inflammation and airway remodelling is central to disease pathophysiology and is related to airway dysfunction (1, 2). With ~300 million people affected and 250,000 annual deaths, asthma significantly contributes to the global health burden (3). Initially, it was considered to be primarily an allergic, eosinophilic Th2 biased disease with involvement of its cytokines (IL-4, IL-5 and IL-13) in the inflammatory cascade leading to allergic exacerbations (4). However, there are non-Th2 asthma patho- phenotypes, where cells like Th17, Th1 and their respective cytokines play a major role in disease pathogenesis and severity (5, 6). Corticosteroids that modulate Th2 cytokines and associated inflammation continue to be the mainstay therapy for the treatment of Th2 dependent allergic asthma (6, 8). The non-Th2 severe asthma cases however are steroid non-responsive with increased risk of exacerbations and morbidity (5, 6). Although

severe asthma accounts for 10-15% of all patients, they consume much more higher cost in healthcare management than acute asthma (3).

Elevated hypoxic response has been reported in more than 90% of severe asthma exacerbations with increased asthma severity and inflammation (7–10). This exaggerated hypoxic response is highly proinflammatory and primarily mediated through inhibition of the oxygen sensor, PHD2 resulting in elevation on HIF-1α (11–14). In addition, neutrophil survival and IL-17-producing CD4+ T helper cell (Th17) levels are known to be induced by HIF-1α (15, 16). High levels of both IL-17 and neutrophils are observed in severe steroid-resistant human asthmatics and mouse models (10, 17–21). A subset of severe asthmatics respond poorly to glucocorticoid treatment, even at a higher dose (3). Modulation of hypoxia signalling or HIF-1α could thus be a promising target to combat the hypoxia-induced severe asthmatic changes. Unfortunately, there is no clinical inhibitor currently available in market that targets HIF-1α.

Plant-derived medicines that have been traditionally used to prevent and treat a large number of diseases are a continuous source of novel drug leads. In India, *Ayurveda* is an ancient system of medicine which offers a translational framework to connect physio-pathology with therapeutics in a stratified manner. The actions of drugs are described on the basis of their effect on biological axes governed by three physiological entities doshas namely *Vata*, *Pitta* and *Kapha* (22) that not only govern homeostasis in individuals but the same when perturbed from their threshold levels, result in disease conditions. Previously we have shown inter-individual variability in genetic as well as expression level in PHD2 between constitution types that differ in *Pitta* (P) and *Kapha* (K) (23, 24). Modulation of this axis revealed hypoxia to be an important modifier of asthma severity (11). We hypothesised that herbal medicines that are reported for the treatment of asthma through balancing of P-K perturbations may have hypoxic modulatory activity. This could then be harnessed to reverse the severe asthma patho-phenotype.

In this study, we have tested the effect of *Adhatoda Vasica* (AV), commonly known as Malabar nut, an ayurvedic medicine indigenously used to treat various aspects of asthma. AV is from *Acanthaceae* family, a dense shrub founds in all parts of India. It has a bitter and astringent taste with *Pitta-Kapha* balancing action, and described for the treatment of asthma and respiratory conditions. Vasicine and vasicinone from AV have been shown to have strong bronchodilatory and anti-inflammatory effects (25–27). In this study, we demonstrated that oral administration of aqueous extract of AV to the Ova-induced allergic mice reduces the cardinal features of asthma both at phenotypic as well as a molecular level. We also provide evidence for the mechanism of action of AV in asthma through modulation of the cellular hypoxic response. We observed that AV treatment to the asthmatic mice inhibits the increased hypoxic response by downregulating HIF-1α. Decline in HIF-1α also improved mitochondrial morphofunction. We further demonstrate that

AV has therapeutic effect even in severe asthma condition that is augmented in mice by elevated hypoxic response and is non-responsive to steroids.

Results

AV attenuates airway pathophysiology of acute allergic lung inflammation in mouse model: We first measured the therapeutic effects of AV extract (fig. S1A) on the pathophysiological features observed in mouse models of acute allergic airway inflammation. A schematic showing the timeline of model development and drug/vehicle treatments is shown in fig. 1A. Mice sensitized and challenged with OVA exhibited increased airway resistance and eosinophilic infiltration into the lungs, mucus metaplasia, and airway remodelling which were reversed by dexamethasone or AV treatment (fig. 1). However, the beneficial effects of AV were found to be non-linear in the range of doses tested (fig. S1). While 130 mg/Kg (AV-D2) dose was found to reverse all the aforementioned pathophysiological features, considerable variability was observed in lower and higher doses (fig. 1, S1). For instance, OVA-induced increase in airway resistance was found to be reduced by all except the highest AV dose (fig. S1B). But, histological assessment of fixed lung sections showed that AV-D2 is more effective in reducing lung inflammation (fig. 1C, F and S1C, F), mucus metaplasia (fig. 1D, G and S1D, G), and sub-epithelial collagen deposition (fig. 1E, H and S1E, H), compare to other doses. Assessment of eosinophils in BAL fluid and TGF-β levels in lung homogenate substantiate efficacy of AV-D2 compared to other doses (fig. 1I, J and S1I, J). In contrast, all the AV doses considered were found to significantly reduce the lung levels of Th2 cytokines, IL-4, IL-5 and IL-13 (fig. 1K and Table S3). Taken together, AV-D2 is more effective, compared to other doses, in the remission of OVA-induced pathological features.

Increased cellular hypoxia (HIF-1α) levels in are reduced after AV treatment both *in vivo* and *in vitro*

An earlier study by our group has shown that the differential severity of airway inflammation in allergic asthma could be modulated by prolyl hydroxylase 2 (PHD2), an inhibitor of HIF-1α which govern the hypoxia axis (11). Exaggerated hypoxic response causes increase in disease severity in acute Ova allergic mice (10, 11). We wanted to explore whether AV treatment could modulate the hypoxia response in Ova challenged mice. We observed elevated levels of HIF-1α in Ova allergic mice compared to Sham mice (fig. 2A, B and C). While dexamethasone treatment failed to restore the OVA-induced increase in HIF-1α levels, AV-D2 completely reversed the HIF-1α levels (fig. 2A, B and C). We observed a non-linear effect of increasing doses of AV on the HIF-1α levels similar to those observed in the previous results (fig. S2A, B). In fact, a strong positive correlation (R_2 = 0.63) was found between airway inflammation score and HIF-1α levels in D0, D2, and D4 doses of AV (fig. S2C). Further, AV also restored the *PHD2* mRNA levels which was

reduced in Ova mice lungs (S2D). In order to confirm the inhibitory effect of AV on HIF-1α as observed in Ova allergic mice, we tested its effect on chemically induced hypoxia in human bronchial epithelial cells (BEAS2B). To induce cellular hypoxia, dimethyloxaloylglycine (DMOG), an inhibitor of PHD and FIH, was used. We observed that *in vitro* treatment of AV (10μg/ml) was capable of attenuating the DMOG induced increase in HIF-1α levels in BEAS2B cells (fig. 2D, S2E). This result confirms the inhibitory effect of AV on HIF-1α levels in cellular hypoxia conditions like asthma. This result confirms the inhibitory effect of AV on HIF-1α levels in cellular hypoxia conditions like asthma and indicates this could be its most important therapeutic effect.

Hypoxia induced mitochondrial dysfunction is rescued by AV treatment

Hypoxia induced mitochondrial dysfunction in asthma has been reported earlier (28, 29). Therefore, we determined the effect of AV on mitochondrial health, since it was observed that AV treatment reduces the increased hypoxia/HIF-1α levels, both *in vitro* as well as *in vivo* conditions. Induction of cellular hypoxia in human bronchial epithelial cells (BEAS2B) by DMOG led to an overall decrease in OCR (fig. 2E) as well as mitochondrial basal respiration, ATP production and maximum respiration. We observed similar results using adenocarcinomic human alveolar basal epithelial cells (A549), where we see AV has potential to improve mitochondrial health in both the cells, when compared to vehicle group as well as in cellular hypoxic environment (fig. 2E and S3A). We next examined effect of cellular hypoxia stress on mitochondrial morphology in BEAS2B cells transfected with mitochondria- targeted green fluorescent protein (mito-GFP). To assess the alterations in mitochondria morphology, previously reported parameters such as number of individual mitochondria, area, elongation, number of networks, and mean branch length of networks were determined. Healthy mitochondria are elongated and exhibit branched chain (network) morphology. In control (vehicle group), the scores for all the aforementioned morphological parameters were found to be higher than in the DMOG treated cells (fig. 2F, G and S2F-I). AV treatment was found to restore morphological defects induced by DMOG treatment (fig. 2F, G and S2F-I) In contrast, Dex treatment alone was found to be ineffective in restoring the DMOG induced morphological alteration in mitochondria (fig. 2F, G and S2F-I), but combination of Dex with AV was observed to be beneficial in significantly improving majority of the morphological parameters measured (fig. 2F, G and S2F-I). This suggests AV treatment may be helpful in conditions where hypoxia stress is prominent through its ability to restore mitochondrial morphofunction. To further validate the effect of AV on mitochondrial morphology, we labeled the mitochondria with mitochondria specific TOM20 (mitochondrial import receptor subunit) antibody in BEAS2B cells treated with DMOG or vehicle. We observed significant impact in improving mitochondrial morphofunction (fig. S3B) after hypoxic stress. Noteworthy, this alteration in mitochondrial parameters after cellular hypoxia was not restored with Dex treatment (fig. S3C-F). However,

combination of Dex with AV treatment in cellular hypoxic stress is able to restore some of the changes in morphological aspects of mitochondria as shown in fig. S3C-F.These results establish that AV targets hypoxia-oxo/nitrative stress-mitochondrial dysfunction axis to attenuate the airway pathology during asthma.

Severe airway inflammation resistant to steroid is resolved with AV treatment

DHB induced severe asthma model

Increased hypoxic response has been associated with increased Th17 cell proliferation as well as neutrophil levels in human asthmatics and murine models leading to steroid resistant phenotype (9–11, 15–20). Earlier, we showed that chemical as well as siRNA-mediated inhibition of prolyl-hydroxylase 2 (PHD-2) in allergic mice led to increased hypoxic response and was associated with severity of the disease (11). In this study, we used the same model of severe asthma to identify their steroid sensitivity (fig. 3A). We found that chemical inhibition of prolyl-hydroxylase (PHD) level in Ova-allergic mice by DHB (10mg/kg,) treatment led to severe increase in airway hyper-responsiveness (AHR) compared to mice challenged with OVA alone and this increased AHR was resistant to Dex treatment (fig. 3B). Therapeutic treatment of AV (130mg/kg, AV-D2) to such DHB+Ova mice led to significant reduction in airway resistance as compared to Ova+DHB and Ova+DHB+Dex mice group (fig. 3B). Similarly, DHB treatment also led to severe increase in airway inflammation (AI) and mucus metaplasia in mice (fig. 3C, G) which was confirmed by quantitative scoring and morphometry of mouse lung sections (fig. S4A, B). This increased AI and mucus metaplasia was resistant to Dex treatment but AV was able to rescue these features (fig. 3C, G and S4A, B). DHB treatment to Ova mice also leads to significant increase in IL-13 levels, which was significantly reduced after AV-D2 treatment and was unaffected by Dex treatment in Ova+DHB mice (fig.S4C). To confirm whether the observed steroid insensitive effect in mice was because of increase in hypoxia and/or HIF-1αlevel, we determined the effect of DHB on HIF-1αprotein levels. We observed that DHB treatment to Ova-allergic mice led to significant increase in lung HIF-1αlevels compared to Ova mice (fig. 3D) which was significantly reduced with AV treatment but not by Dex treatment (fig. 3D). In addition, cellular hypoxia induced by DHB treatment leads to significant increase in steroid non-responsive and steroid resistant asthma associated cytokines namely IL-17A (fig.3E), KC (fig.3F, mouse homologue of IL-8), IFN-γ and TNF-α(fig. S4D, E), compared to Ova mice group. These increased cytokine levels were also significantly reduced with AV treatment whereas Dex treatment (fig. 3 D-F and S4D, E) couldn't reduce them. In addition, there was also a significant difference in therapeutic effect accounted by AV-D2 treatment on DHB induced severe airway inflammation when compared with the Dex-treated severe asthmatic mice

(Ova+DHB+Dex). These results indicate that therapeutic treatment of AV to severe allergic mice reduces airway inflammation and associated cytokine levels through modulation of HIF-1αlevels.

PHD2 siRNA induced severe asthma model

In order to test whether AV alleviates the steroids resistance under high cellular hypoxia in the severe asthma through specific inhibition of PHD2 in lung, we administered siRNA through intranasal route in Ova allergic mice (fig. 4A). Down-regulation of PHD2 level was confirmed by measurements of its protein levels (fig. 4B). Interestingly AV treatment increases the PHD2 protein levels significantly compared to only PHD2 siRNA administered allergic mice (fig. 4B).Consequently, a significant increase in HIF-1α was also observed in PHD2 siRNA treated Ova mice compared to scrambled (Scrm)siRNA+Ova mice group and increased HIF-1α was significantly downregulated by AV treatment but not by Dex (fig. 4C). PHD2 siRNA recapitulated the severely increased airway resistance, which was significantly reduced after AV (130mg/kg, AV-D2) treatment but not by Dex treatment (fig. 4D). PHD2 siRNA treatment to Ova mice also increased the airway inflammation (AI), mucus metaplasia as well as IL-17A levels significantly compared to Scrm siRNA treated Ova mice (fig. 4E, F and S5A, B and F). These increased levels of AI and IL-17A was significantly reduced in AV but not in Dex treatment (fig. 4E, F and S5A, B). In addition, PHD2 siRNA treatment also increases the pro-inflammatory and steroid resistant related cytokines like IL-13, KC and IL-6 levels (fig. S5C-E). Oral administration of AV-D2 to such a severe asthmatic mice reduces these elevated levels of cytokines but not by Dex treatment (fig. S5C-E). This confirms that the observed severe asthmatic features in mice is because of increase in cellular hypoxic response in allergic mouse lung and it could be attenuated by AV administration. This effect could be possibly increasing lung PHD2 levels. These results indicate that AV reduces the severe steroid resistant airway inflammation in mice with exaggerated hypoxic response.

Discussion

Plant derived medicines, like phytoextracts, form an integral component of indigenous medical systems and have been successfully used to prevent and treat various diseases (30–32). In this study, we use aqueous extract of the plant *Adhatoda Vasica* (AV) which was prepared as per descriptions in *Ayurvedic* texts to understand its effect and possible mode of action against asthma (33–35). AV is one of the primary medicinal herbs in *Ayurveda* for the treatment of cough, bronchitis, asthma and various respiratory ailments (27). A number of active constituents have been isolated from AV herb, among which vasicine and vasicinone are the primary alkaloids and known to have strong bronchodilatory effects (25, 27). Semisynthetic derivatives of vasicine, bromohexine and ambroxol, are also widely used either alone or in combination with expectorant and mucolytic agents. (36). We observed, therapeutic administration of AV has a strong inhibitory action against increased airway resistance and airway inflammation observed in Ova challenged allergic mice (fig.

1). Though the therapeutic effects on the cardinal features of asthma like airway hyperresponsiveness (AHR) and airway inflammation (AI) was observed nearly at all four doses, of AV, the D2 dose was found to be most effective across all parameters with least variability within the group. Its effect on cytokine levels was dose-independent and all the doses were more or less equally effective in reducing Th2 and Th17 cytokines (table S3 and fig. S1F). However, AV demonstrated a "U-shape curve effect" observable at the level of airway physiology as evident in AHR (fig. S1C.) as well as AI (fig. 1F) and, in airway remodelling (fig. S1D, E) mediated by increased TGF-β1 in allergic mice (fig. 1H). This U shaped curve effect was mirrored in HIF-1α levels indicating the role of AV as a modulator of hypoxic response (fig. 2A).

A modifying role of elevated hypoxic response in acute allergic asthma primarily mediated through hypoxia inducible factor-1α (HIF-1α) has been shown by our group earlier(11). Mild or low level of cellular hypoxia mediated by PHD2 inhibition produces the protective effect in allergic asthma whereas, high hypoxia level induces exaggerated pro-inflammatory and pro-asthmatic effects in allergic mice (11). Levels of IL-17A (a Th17 cytokine) and neutrophils are known to positively regulated by HIF-1α and both IL-17A and neutrophils are high in severe steroid resistant human asthmatics and mouse models (9–11, 15–20).

We therefore examined the effect of PHD inhibition and hypoxia response for steroid sensitivity as well the effects of AV on hypoxia induced severe asthma model. Here, we show that chemical as well as siRNA mediated induction of HIF-1α in allergic mice increases the asthma severity (fig. 3, 4). We also show that AV treatment is able to rescue all the severe asthma phenotypes including its effect on molecular markers like IL17, KC which were found to be non-responsive to the steroids (Dex) (fig. 3, 4, S4 and S5). This could be because of inhibitory effect of AV on increased HIF-1α levels or by restoration of decreased PHD2 levels in allergic severe asthmatic mice (fig. 4B, S2C). The inhibitory effect of AV on HIF-1α in cellular hypoxic condition is also validated by *in vitro* experiments (fig. 2D, S2D).

One of the axes associated with severe inflammation is hypoxia-oxo-nitrative stress-mitochondrial dysfunction in asthma (28, 29, 37, 38). Indeed, increased cellular hypoxic response have been shown to cause mitochondrial dysfunction and oxidative stress, both of which have larger role in pathogenesis of asthma (28, 38). Coupled with our *in vitro* results we thought it would be worthwhile to check if AV could improve the consequences of hypoxia such as mitochondrial dysfunction and thereby modulate the outcomes of the disease. Hypoxia induced mitochondrial dysfunction was assessed *in vitro* in cultured lung epithelial cells treated with DMOG. Our results reveal that AV treatment to lung epithelial cells in hypoxic conditions was able to improve the mitochondrial dysfunction revealed through mitochondrial morphological analysis and increased OCR (fig. 2E-G, S2E-I and S3). AV treatment restored the thread like shape and mitochondrial network morphology caused by cellular hypoxic stress (fig. 2E-G, S2E-I and S3). The beneficial effects of AV on

mitochondrial respiration could be either through direct attenuation of cellular hypoxic state or indirectly through increase in mitochondrial biogenesis (37). It would be interesting to test the effect of AV in corticosteroid insensitive obese-asthma phenotype, where the mitochondrial dysfunction and hypoxia co-exist (29).

Inter-individual variability in baseline levels of HIF-1α and/ or PHD2 may predispose individuals to severe hypoxia response in respiratory disorders. Previously, we observed genetic variation in *PHD2* in healthy individuals linked to *Ayurveda* constitution types was different between natives of high altitude and sojourners who suffered from HAPE (24). Subsequently we showed the significance of PHD2 in asthma, where chemical inhibition of PHD2 modulated hypoxic response in asthma and increases disease severity (11). *Ayurveda*, an Indian system of medicine, describes inter-individual variability in health and disease through common organising principle of *Tridosha,* i.e. *Vata Pitta* and *Kapha*. *Tridosha* are three physiological entities which govern the functioning and homeostasis of the system, which have been shown to have the molecular correlation (22, 23, 39–42). The drugs prescribed in *Ayurveda* are also classified on the basis of their effect on *Tridosha* (43). The herbal medicine *Adhatoda Vasica* tested in this study is described to be *Pitta- Kapha* balancing herb and used for treatment of asthma and other respiratory conditions (43). Effect of AV on asthma not only lead to identification of novel inhibitor of HIF-1α, that could be useful in treatment of severe asthma, but also explains/validates the molecular correlate of *Pitta- Kapha* axis identified through the inter-individual variability between *Pitta- Kapha* constitution types using *Ayurgenomics* approach.

Taken together, we demonstrate for the first time that the inhibition of increased HIF-1α is an important therapeutic mechanism of *Adhatoda Vasica* effects. It is also observed that the effect of AV is not limited to acute asthma, but also beneficial in severe asthma model where steroids are ineffective. In addition, AV also showed a promising effect against mitochondrial dysfunction in elevated cellular hypoxia state. As we described, the extract (fig. S1A and table S1) used in this study is a mixture of various quinazoline alkaloids (Vasicine, Vasicinone, Adhavasicinone etc.), it is possible that AV may be acting on molecular targets or processes other than HIF-1α, for the observed anti-asthmatic effects. Nevertheless, results of our study highlights an important molecular mechanism that could explain the clinical efficacy of aqueous AV extract reported in human asthmatic patients (33, 34). Also, anti-inflammatory effects of AV observed in acute asthma models indicate that AV could be an alternative to steroids which has multiple local and systemic side effects. This study demonstrates the potential of AV treatment specifically in severe steroid resistant asthmatics and in conditions where restoration of mitochondrial dysfunction is pertinent. The therapeutic observation of AV extract on cellular, histological (tissue level) and physiological (phenotype level) parameters involved in pathophysiology reflects the importance of retaining the multi compound nature of the extract as practised in *Ayurveda*.

Materials and Methods

AV was prepared according to the classical method described for *rasakriya* (decoction-condensation- drying) in *Caraka Samhita* (33, 44). The detailed quality and chemical fingerprinting study were carried out by LC-MS at CSIR-CDRI, Lucknow, India (fig. S1A, B and table S1, S2). Acute allergic asthma was developed in mice using Ova sensitization by intraperitoneal injection from a 1-3 week. After a 1week gap mice were challenged with Ova using an aerosol nebulizer for 7 days. AV (13-260mg/kg, orally), and Dex (0.75mg/kg, orally) was given for 4 days from the 24th-day protocol. On the 28th-day, mice were cannulated to determine airway resistance in response to methacholine and sacrificed by phenobarbital anesthesia. Severe asthma model was developed by intraperitoneal injection of DHB (10 mg/kg), and intranasal PHD2 siRNA (90 µg) treatment to induce a hypoxic response in Ova-sensitized and challenged mice. Lungs were removed, fixed in formalin, embedded in paraffin, and sectioned at 5µm. Staining of hematoxylin and eosin, periodic acid-Schiff, and Masson Trichrome was used to assess the lung inflammation, mucus hypersecretion, and sub-epithelial fibrosis, respectively. Quantitative real-time reverse transcription PCR (RT-PCR) was used to quantify PHD2 mRNA expression. Lung tissue lysate was used for cytokines and western blot assay. Cellular hypoxia model was developed using DMOG (1mM; 32 hours), in BEAS2B and A549 lung epithelial cells. AV(10µg/ml), and Dex (10µM/ml) were added to culture after 8 hours of DMOG induction and kept for next 24 hours. The cell lysate was used to detect HIF-1α protein. Seahorse assay was carried out using a 24-well plate with BEAS-2B, and A549 cell culture in presence of DMOG. GFP-mito or immunofluorescence was used to detect mitochondria and its morphological characteristics. Data were analyzed by one- or two-way analysis of variance (ANOVA), Student's t-test, and correlation analysis. Mitochondrial quantitative analysis was performed by using image J. The difference was considered to be statistically significant when $P< 0.05$.

Details of methods and experimental protocol is provided in supplementary materials and methods.

Acknowledgments

We acknowledge animal house and imaging department for access to facility. We thank Dr. Ramniwas Prasher for his valuable suggestions regarding AV extract preparation and its use in clinical terms of *Ayurveda*. We also thank Dr. Balaram Ghosh, Dr. Ullagnath Mabalirajan , Dr. Krishnendu Chakroborty and Dr. Soumya Sinha Roy for discussion and suggestions in study. AG, LP and KK acknowledge AcSIR (Academy of Scientific and Innovative Research) for PhD. registrations and CSIR (Council of Scientific and Industrial Research) for fellowship. **Funding:** This work is supported by grant to CSIR-TRISUTRA (MLP-901) from the CSIR and Center of Excellence grant by Ministry of AYUSH, Govt. of India.

Author Contributions

A.G. designed and performed the experiment, analysed the results and wrote the paper. A.G., L.P., and K.K. performed the experiment, analysed the results. V.J. and V.P.S. contributed to animal model experiments. N.K.B. contributed in seahorse experiment and quantification of flurosense labeled mitochondrial images. S.S. & M.K. contributed in imaging experiment. B.P. conceptualized the study, provided AV, quality control information, discussion, designed the experiment, analysed the results and wrote the paper. M.M. and A.A. designed experiments, analysed and discussed the results and wrote the paper. All the authors reviewed and approved the final version of the manuscript.

References

1. A. Papi, C. Brightling, S. E. Pedersen, H. K. Reddel, Asthma. *Lancet (London, England)* **391**, 783–800 (2018).

2. S. T. Holgate, Innate and adaptive immune responses in asthma. *Nat. Med.* **18**, 673–683 (2012).

3. J. T. Olin, M. E. Wechsler, Asthma: pathogenesis and novel drugs for treatment. *BMJ* **349**, g5517 (2014).

4. G. P. Anderson, Endotyping asthma: new insights into key pathogenic mechanisms in a complex, heterogeneous disease. *Lancet (London, England)* **372**, 1107–19 (2008).

5. S. E. Wenzel, Asthma phenotypes: the evolution from clinical to molecular approaches. *Nat. Med.* **18**, 716–725 (2012).

6. J. V Fahy, Type 2 inflammation in asthma--present in most, absent in many. *Nat. Rev. Immunol.* **15**, 57–65 (2015).

7. E. Ballester, *et al.*, Ventilation-perfusion mismatching in acute severe asthma: effects of salbutamol and 100% oxygen. *Thorax* **44**, 258–67 (1989).

8. R. Rodriguez-Roisin, Acute severe asthma: pathophysiology and pathobiology of gas exchange abnormalities. *Eur. Respir. J.* **10**, 1359–71 (1997).

9. C. E. Charron, *et al.*, Hypoxia-inducible factor 1alpha induces corticosteroid-insensitive inflammation via reduction of histone deacetylase-2 transcription. *J. Biol. Chem.* **284**, 36047–54 (2009).

10. K. J. Baek, *et al.*, Hypoxia potentiates allergen induction of HIF-1α, chemokines, airway inflammation, TGF-β1, and airway remodeling in a mouse model. *Clin. Immunol.* **147**, 27–37 (2013).

11. T. Ahmad, *et al.*, Hypoxia Response in Asthma. *Am. J. Respir. Cell Mol. Biol.* **47**, 1–10 (2012).

12. L. E. Crotty Alexander, *et al.*, Myeloid cell HIF-1α regulates asthma airway resistance and eosinophil function. *J. Mol. Med.* **91**, 637–644 (2013).

13. C. Matrone, *et al.*, HIF-1alpha reveals a binding activity to the promoter of iNOS gene after permanent middle cerebral artery occlusion. *J. Neurochem.* **90**, 368–378 (2004).

14. Y. Saini, *et al.*, Role of hypoxia-inducible factor 1{alpha} in modulating cobalt-induced lung inflammation. *Am. J. Physiol. Lung Cell. Mol. Physiol.* **298**, L139-47 (2010).

15. E. V. Dang, *et al.*, Control of TH17/Treg Balance by Hypoxia-Inducible Factor 1. *Cell* **146**, 772–784 (2011).

16. S. R. Walmsley, *et al.*, Hypoxia-induced neutrophil survival is mediated by HIF-1alpha-dependent NF-kappaB activity. *J. Exp. Med.* **201**, 105–15 (2005).

17. L. McKinley, *et al.*, TH17 cells mediate steroid-resistant airway inflammation and airway hyperresponsiveness in mice. *J. Immunol.* **181**, 4089–97 (2008).

18. J. Chesné, *et al.*, IL-17 in Severe Asthma. Where Do We Stand? *Am. J. Respir. Crit. Care Med.* **190**, 1094–1101 (2014).

19. L. Panda, *et al.*, Linoleic acid metabolite leads to steroid resistant asthma features partially through NF-κB. *Sci. Rep.* **7**, 9565 (2017).

20. R. H. Green, *et al.*, Analysis of induced sputum in adults with asthma: identification of subgroup with isolated sputum neutrophilia and poor response to inhaled corticosteroids. *Thorax* **57**, 875–9 (2002).

21. W. C. Moore, *et al.*, Sputum neutrophil counts are associated with more severe asthma phenotypes using cluster analysis. *J. Allergy Clin. Immunol.* **133**, 1557–63.e5 (2014).

22. B. Prasher, G. Gibson, M. Mukerji, Genomic insights into ayurvedic and western approaches to personalized medicine. *J. Genet.* **95**, 209–28 (2016).

23. B. Prasher, *et al.*, Whole genome expression and biochemical correlates of extreme constitutional types defined in Ayurveda. *J. Transl. Med.* **6**, 48 (2008).

24. S. Aggarwal, *et al.*, EGLN1 involvement in high-altitude adaptation revealed through genetic analysis of extreme constitution types defined in Ayurveda. *Proc. Natl. Acad. Sci.* **107**, 18961–18966 (2010).

25. A. H. AMIN, D. R. MEHTA, A Bronchodilator Alkaloid (Vasicinone) from Adhatoda vasica Nees. *Nature* **184**, 1317–1317 (1959).

26. G. W. CAMBRIDGE, A. B. A. JANSEN, D. A. JARMAN, Bronchodilating Action of Vasicinone and Related Compounds. *Nature* **196**, 1217–1217 (1962).

27. U. P. Claeson, T. Malmfors, G. Wikman, J. G. Bruhn, Adhatoda vasica: a critical review of ethnopharmacological and toxicological data. *J. Ethnopharmacol.* **72**, 1–20 (2000).

28. U. Mabalirajan, *et al.*, Mitochondrial structural changes and dysfunction are associated with experimental allergic asthma. *J. Immunol.* **181**, 3540–8 (2008).

29. U. Mabalirajan, B. Ghosh, Mitochondrial dysfunction in metabolic syndrome and asthma. *J. Allergy* **2013**, 340476 (2013).

30. H.-F. Ji, X.-J. Li, H.-Y. Zhang, Natural products and drug discovery. Can thousands of years of ancient medical knowledge lead us to new and powerful drug combinations in the fight against cancer and dementia? *EMBO Rep.* **10**, 194–200 (2009).

31. A. L. Harvey, R. Edrada-Ebel, R. J. Quinn, The re-emergence of natural products for drug discovery in the genomics era. *Nat. Rev. Drug Discov.* **14**, 111–129 (2015).

32. B. Shen, A New Golden Age of Natural Products Drug Discovery. *Cell* **163**, 1297–300 (2015).

33. R. Prasher, D. Pandey, S. De, B. Ravishankar, Standardization of Vasa Ghrta and its extract form and their comparative Pharmaco-Clinical study with special reference to Swasa Roga. *Ayu* **6** (1999).

34. A. Gupta, P. K. Prajapati, A clinical review of different formulations of Vasa (Adhatoda vasica) on Tamaka Shwasa (asthma). *Ayu* **31**, 520–4 (2010).

35. A. M. Paneliya, B. Patgiri, R. Galib, P. K. Prajapati, Efficacy of Vasa Avaleha and its granules on Tamaka Shwasa (bronchial asthma): Open-label randomized clinical study. *Ayu* **36**, 271–7 (2015).

36. S. Kumar Singh Scholar, *et al.*, A complete over review on Adhatoda vasica a traditional medicinal plants. *J. Med. Plants Stud. JMPS* **175**, 175–180 (2017).

37. B. Pattnaik, *et al.*, IL-4 promotes asymmetric dimethylarginine accumulation, oxo-nitrative stress, and hypoxic response–induced mitochondrial loss in airway epithelial cells. *J. Allergy Clin. Immunol.* **138**, 130-141.e9 (2016).

38. P. H. Reddy, Mitochondrial Dysfunction and Oxidative Stress in Asthma: Implications for Mitochondria-Targeted Antioxidant Therapeutics. *Pharmaceuticals (Basel).* **4**, 429–456 (2011).

39. T. P. Sethi, B. Prasher, M. Mukerji, Ayurgenomics: A New Way of Threading Molecular Variability for Stratified Medicine. *ACS Chem. Biol.* **6**, 875–880 (2011).

40. S. Aggarwal, *et al.*, Combined genetic effects of EGLN1 and VWF modulate thrombotic outcome in hypoxia revealed by Ayurgenomics approach. *J. Transl. Med.* **13** (2015).

41. P. Tiwari, *et al.*, Recapitulation of Ayurveda constitution types by machine learning of phenotypic traits. *PLoS One* **12**, e0185380 (2017).

42. N. S. Chauhan, *et al.*, Western Indian Rural Gut Microbial Diversity in Extreme Prakriti Endo-Phenotypes Reveals Signature Microbes. *Front. Microbiol.* **9**, 118 (2018).

43. S. P., *Charaka Samhita: text with english translation* (Chaukambha Orientalia Publisher, 1981).

44. P. V. Sharma, *Caraka-Samhita: Text with English translation* (1981).

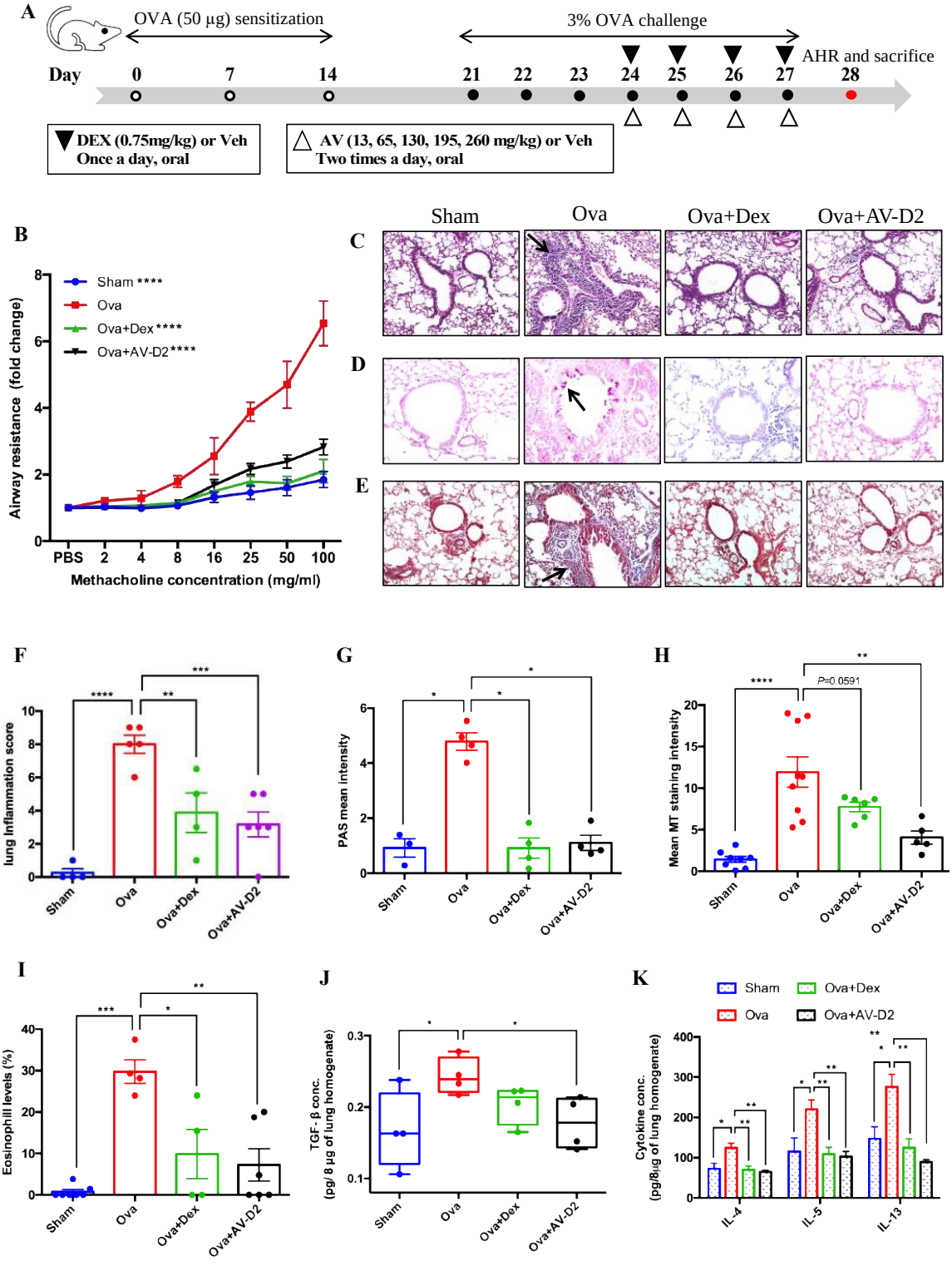

Fig. 1. **AV treatment alleviates the asthmatic features in mice model of acute asthma. (A)** Schematic representation showing the timelines for mice model development and drug treatments. Male BALB/c mice were sensitised and challenged using Ova-allergen and AV or Dex was administered to Ova-allergic mice from day 24 to 27 as described in materials and methods. **(B)** Flexivent analysis of airway resistance after methacholine treatment in AV or Dex treated Ova allergic mice compared with Ova alone mice. **(C to E)** Representative photomicrographs of fixed mouse lung tissue sections stained with (C) H&E (10X magnification), (D) PAS (20X magnification), and (E) MT (10X magnification) for the analysis of cellular infiltration of inflammatory cell, mucin and collagen levels, respectively. Black arrow indicates positive staining in respect to particular stain. **(F)** Quantification of peribronchial and perivascular inflammation of mouse lung tissues stained with H&E in using inflammation grade scoring system. **(G and H)** Densitometric analysis of mouse lung tissues stained with PAS and MT to measure mucus metaplasia and collagen deposition using ImageJ. **(I)** Eosinophil abundance in mouse BAL fluid. (**J and K)** ELISA for TGF-β1 and Th2 cytokines in mice lung homogenate. Data are shown as mean ±SEM of three to seven mice per group and representative from three independent experiments. Significance denoted by *$P \leq 0.05$, **$P \leq 0.01$, ***$P \leq 0.001$ and ****$P \leq 0.000$; by two way ANOVA (B) and ordinary one way ANOVA (F to K). **Ova-** chicken egg albumin, **Sham**- vehicle (PBS), **Dex**- Dexamethasone (0.75mg/kg), AV-**D2**- *Adhatoda Vasica* extract (130 mg/kg)

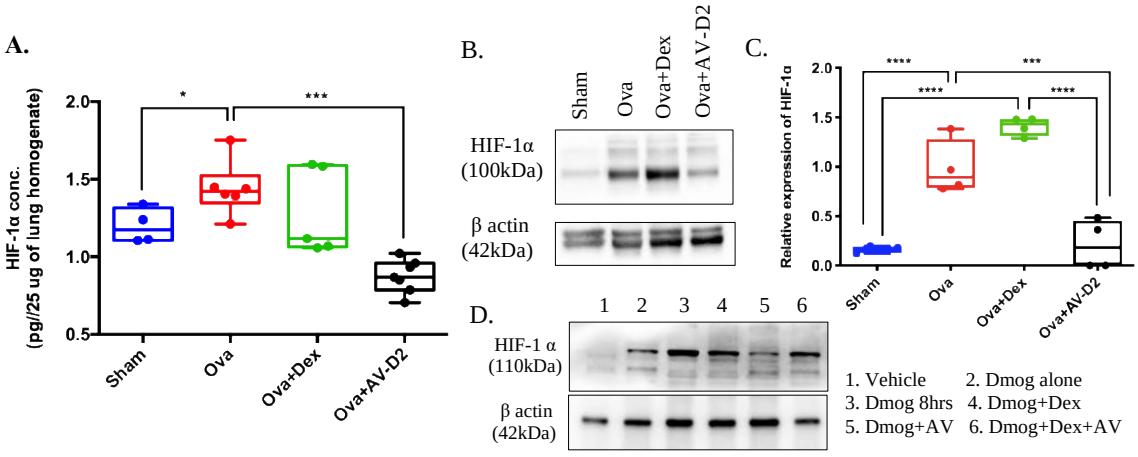

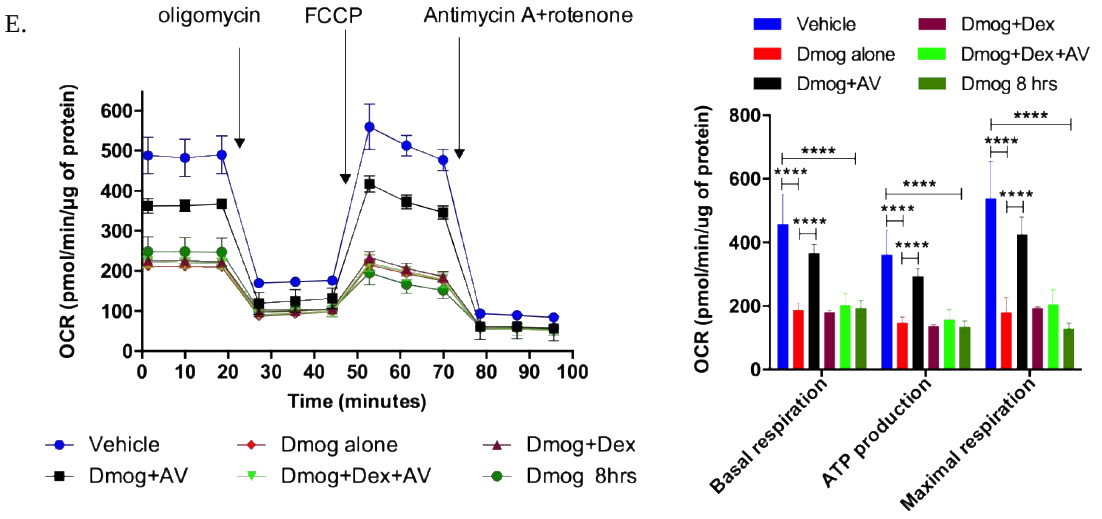

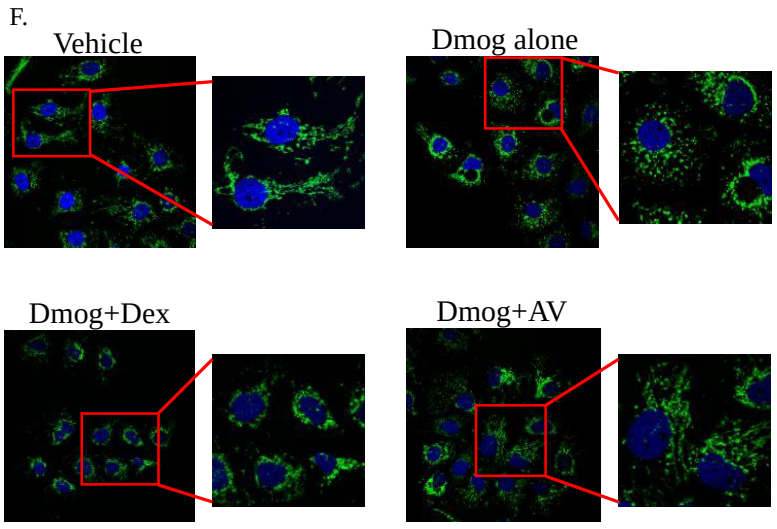

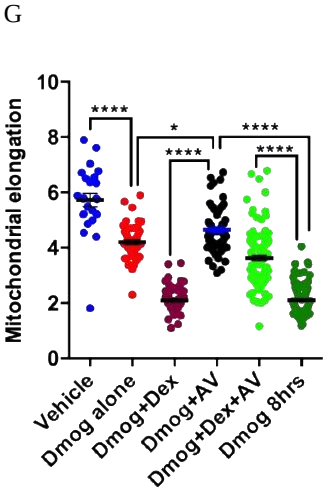

Fig. 2. AV treatment rescues hypoxia induced HIF-1α and related mitochondrial dysfunction. (A to C) HIF-1α levels measured in lung homogenate of acute asthmatic mice by (A) ELISA and (B) Western blot analysis, (C) compiled with densitometric comparison for western blot. Data are shown as mean ±SEM of four to seven mice per group and representative of three independent experiments. (**D)** Representative western blot for HIF-1α abundance in BEAS2B cell lysate. (**E to G**) Effect of AV on cellular hypoxia induced mitochondrial dysfunction. (E) Left: representative OCR graph showing effect of cellular hypoxia on mitochondrial bioenergetics profile in presence of AV or Dex treatment. Right: mitochondrial bioenergetics profile measured at Basal respiration, ATP production and at Maximum respiration level in presence of ETC inhibitors. Cellular hypoxia-induced changes in mitochondrial morphology. (F) Representative confocal images showing the mitochondria in BEAS2B cells transfected with mitochondria targeted-GFP (mito-GFP) and nucleus stained with blue (DAPI). Boxed areas of image are shown with magnification to represent the morphological status of mitochondria typical to the treatment or specific condition. (G) Dot plot showing mitochondrial elongation parameter. Data are shown as mean ±SEM of thirty or more cells per group and representative of at least two independent experiments. Significance denoted by *$P \leq 0.05$, **$P \leq 0.01$, ***$P \leq 0.001$ and ****$P \leq 0.0001$; by Unpaired t test with Welch's correction (A), ordinary one way ANOVA (B), two way ANOVA with Tukey's multiple correction test (E), ordinary one way ANOVA with Tukey's multiple correction test (G). **Ova-** chicken egg albumin, **Sham**- vehicle (PBS), **Dex**- Dexamethasone (0.75mg/kg), **AV-D2**- *Adhatoda Vasica* extract (130 mg/kg), **BEAS-2B**- normal human bronchial epithelium cells, **OCR**- oxygen consumption rate, **DMOG**- dimethyloxaloylglycine, **DMOG+AV**- DMOG+10µg/ml. *Adhatoda Vasica* extract, **DMOG+Dex**- DMOG+10nM of Dexamethasone, **DMOG+Dex+AV**-DMOG+10nM of Dexamethasone+10µg/ml. *Adhatoda Vasica* extract, **DMOG 8hrs**- DMOG treatment for 8 hours.

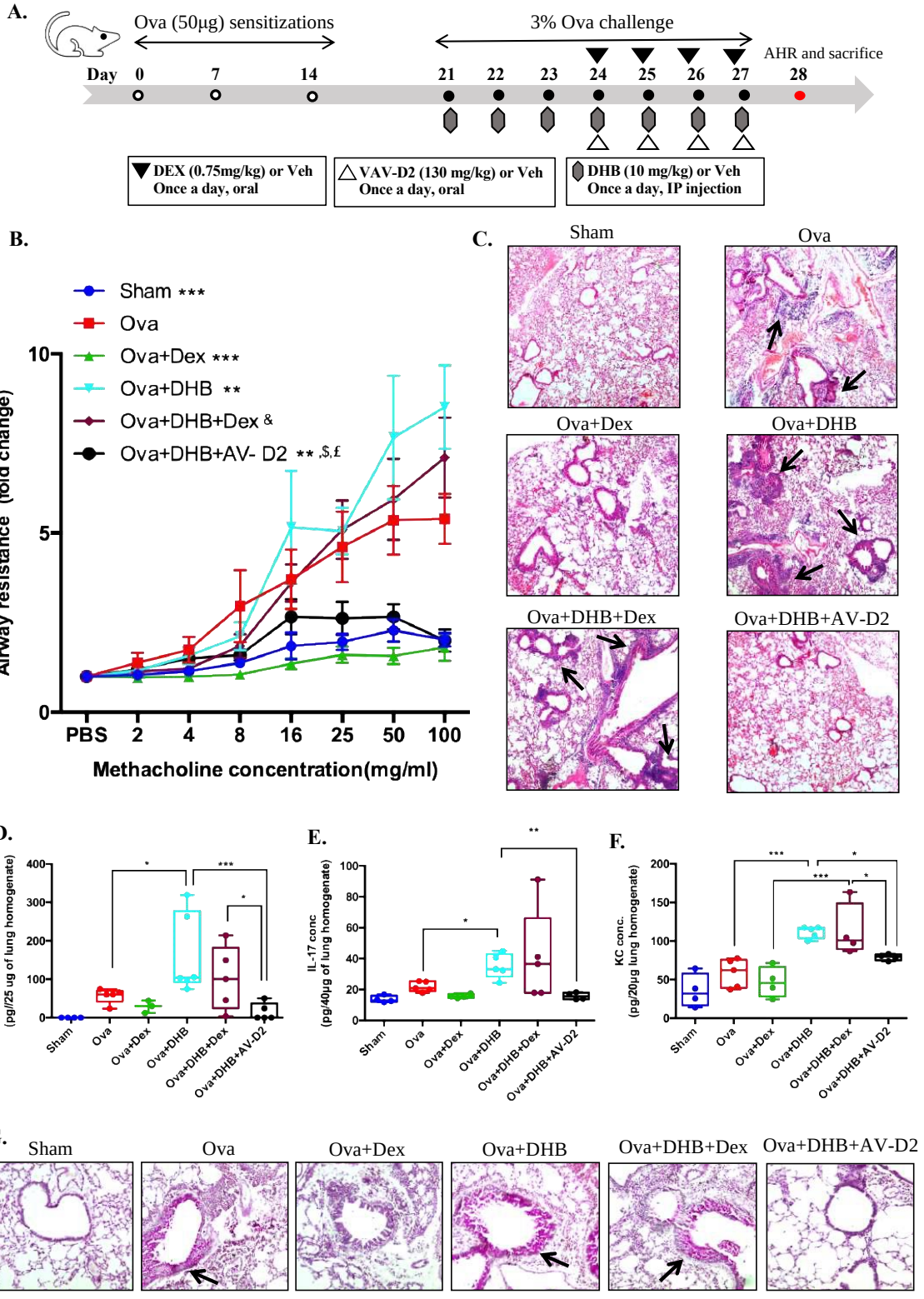

Fig. 3. AV treatment resolves the severe steroid resistant airway pathological features induced by chemical inhibition of PHD in mice model of asthma. (A) Schematic representation of experimental protocol used to induce severe asthma in mice using DHB as described in materials and methods. **(B)** Flexivent analysis of airway resistance after methacholine treatment for DHB induced severe asthma mouse model. (**C)** Representative photomicrographs (4X magnification) of mouse lung tissues stained with H&E **(D to F)** ELISA analysis for HIF-1α (D), IL-17 (E) and KC (F) abundance in mouse lung tissue homogenate. **(G)** Representative photomicrographs of mouse lung tissues stained with PAS. Arrow indicates positive staining for mucin. Data are shown as mean ±SEM of three to five mice per group and representative of two independent experiment. Significance denoted by *$P \leq 0.05$, **$P \leq 0.01$, ***$P \leq 0.001$ and ****$P \leq 0.0001$ compared with Ova group, & denotes $P \leq 0.0001$ compared to Ova+Dex group, $ and £ denotes $P \leq 0.0001$compared to Ova+DHB group and Ova+DHB+Dex group respectively; assessed by two way ANOVA with Tukey's multiple correction test (B), ordinary one way ANOVA (D and F), Unpaired t test with Welch's correction (E). **Ova-** chicken egg albumin, **Sham**- vehicle (PBS), **DHB**- ethyl, 3,4 -dihydroxy benzoic acid (10mg/kg), **Dex**- Dexamethasone (0.75mg/kg), **AV-D2**- *Adhatoda Vasica* extract (130mg/kg).

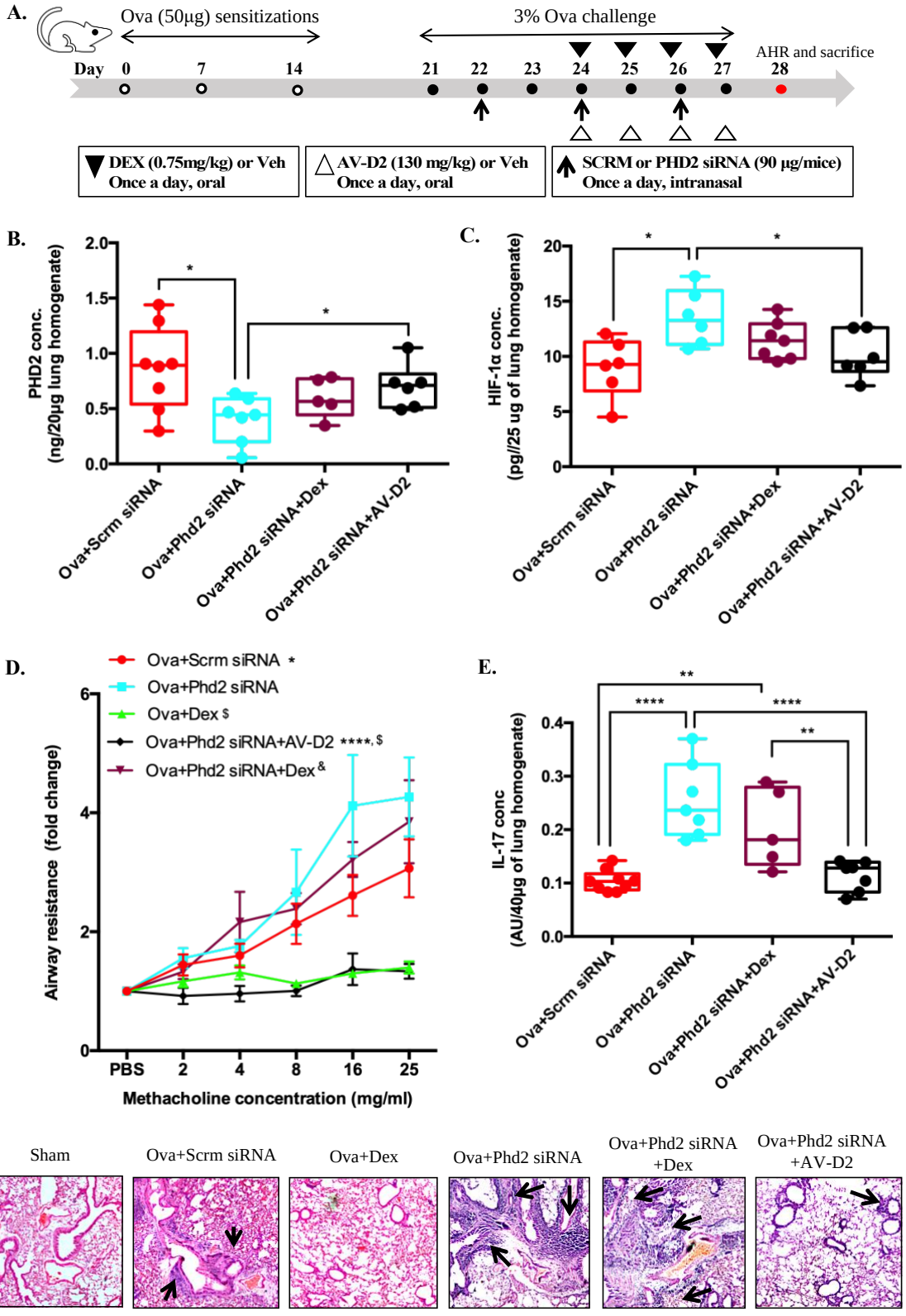

Fig. 4. AV treatment rescues the *PHD2* siRNA induced severe steroid insensitive asthmatic features in mouse model of asthma. A) Schematic representation of experimental protocol used to induce severe asthma in mice using *PHD2* siRNA as described in materials and methods. **(B and C)** ELISA analysis for PHD2 (B) and HIF-1α (C) levels in mouse lung tissue homogenate. **(D)** Flexivent analysis of airway resistance after methacholine treatment in *PHD2* siRNA mediated severe asthma mouse model. **D)** ELISA analysis for IL-17 abundance in mouse lung tissue homogenate. **(E)** Representative photomicrographs (4X magnification) of mouse lung tissues stained with H&E. Black arrow indicates airway inflammation. Data are shown as mean ±SEM of five to nine mice per group and representative of two independent experiment. Significance denoted by **P* ≤0.05, and *****P*≤0.0001compared with Ova+PHD2 siRNA mice, £ denotes *P* ≤0.05 compared to Ova+Scrm siRNA group, $ indicates *P*≤0.01 compared with Ova+PHD2 siRNA+Dex group and & denotes *P*≤0.0001compared with Ova+Dex group; assessed by assessed by Unpaired t test with Welch's correction (B and C), two way ANOVA with Tukey's multiple correction test (D), and ordinary one way ANOVA (E). **Ova-** chicken egg albumin, **Sham**- vehicle (PBS), **Scrm siRNA**- Scrambled siRNA-90μg/mice, **PHD2 siRNA-** mouse specific PHD2 siRNA 90μg/mice., **Dex**- Dexamethasone (0.75mg/kg), **AV-D2**- *Adhatoda Vasica* extract (130mg/kg).

Supplementary Information for

Adhatoda Vasica ameliorates cellular hypoxia dependent mitochondrial dysfunction in acute and severe asthmatic mice

Atish Gheware, Lipsa Panda, Kritika Khanna, Vaibhav Jain, Naveen Kumar Bhatraju, Shakti Sagar, Manish Kumar, Vijay Pal Singh, Mitali Mukerji, Anurag Agrawal* and Bhavana Prasher*

Supplementary Information Text

Materials and Methods

Preparation of plant extract and LC-MS fingerprinting: *Adhatoda Vasica* (AV) was collected from Delhi-NCR region, India in the flowering season (November to March). Water extract of plant (leaves, twigs and flowers) was prepared according to classical method described for rasakriya in *Caraka Samhita* (1). The process for the formulation involved preparation of decoction condensation and drying as described in earlier study (2). Chemical fingerprinting of prepared AV extract was carried out by LC-MS at CSIR-CDRI, Lucknow, India; in two independent experiment. Briefly, Liquid chromatography-electrospray ionization-mass spectrometry of AV extract was recorded in positive- and negative- ion modes using an Agilent 6520 QTOF-MS/MS system coupled with an Agilent 1200 HPLC (Agilent technologies, USA) via an ESI interface **(Table S1 and S2)**. HPLC separation was carried out on a Supelco Discovery HS C18 column (15 cm×4.6 mm, 3µm) operated at 25°C. The mobile phase, which consisted of a 0.1% formic acid aqueous solution and acetonitrile. The analyses were performed on an Agilent 1200 HPLC system consisted of a quaternary pump (G1311A), online vacuum degasser (G1322A), auto sampler (G1329A), thermostatted column compartment (G1316C) and diode-array detector (G1315D). In the ESI source, nitrogen was used as drying and collision gas in both positive and negative ion mode. Detection was carried out within a mass range of m/z 50-2000 and resolving power above 15000 (FWHM). The chromatographic and mass spectrometric analyses were performed by using Mass Hunter software version B.04.00 build 4.0.479.0 (Agilent Technology, USA).

Animals

All animals were maintained as per the guidelines of the Committee for the Purpose of Control and Supervision of Experiments on Animals (CPCSEA). The BALB/c male mice (8-10 weeks old) were obtained from Central Drug Research Institute, Lucknow, India and were acclimatized to animal house environment one week prior to starting the experiments at CSIR-Institute of Genomics and Integrative Biology (IGIB), Delhi, India; as per the protocols approved by Institutional Animal Ethics

Committee of CSIR-IGIB, Delhi, India. All the surgical procedures were performed under sodium pentobarbital anesthesia and maximum efforts were taken for minimum suffering of animals.

Grouping of mice

Mice were divided into two groups, acute and severe as per allergen challenge and treatment protocol. In both groups, there were three main sub-groups (*n* = 4-7): Sham (mice that were PBS sensitized, PBS challenged), Ova (mice that were Ova [grade V chicken egg Ovalbumin, Sigma] sensitized, Ova challenged and treated with vehicle, 50 % ethanol and distill water), Ova+Dex (allergic mice treated with Dexamethasone [0.75mg/kg], dissolved in 50% ethanol, by orally). In acute model, in addition to the above groups, mice were divided into five different Ova+AV groups (allergic mice treated with *Adhatoda* extract [AV, 13mg/kg, 65mg/kg, 130mg/kg, 195mg/kg and 260mg/kg], dissolved in distil water, oral). For severe model, Ova sensitized and challenged mice were further sub-divided according to treatment: Ova+DHB (allergic mice treated with ethyl 3,4-dihydroxybenzoic acid [DHB, 10 mg/kg], dissolved in 50% ethanol, intraperitoneal injection) or Ova+ scrambled siRNA (mice that were Ova sensitized, Ova challenged and administered with intranasal scrambled siRNA[90 µg]) and Ova+PHD2 siRNA (allergic mice treated with intranasal prolyl hydroxylase domain 2 siRNA and treated with vehicle), Ova+DHB+Dex (allergic mice treated with DHB [10 mg/kg] and administered with Dexamethasone [0.75mg/kg]) or Ova+PHD2+Dex (allergic mice treated with intranasal PHD2 siRNA [90 µg] and administered with Dexamethasone [0.75mg/kg]), Ova+DHB+AV (allergic mice treated with DHB [10 mg/kg] and administered with AV [130 mg/kg] or Ova+PHD2+AV(allergic mice treated with intranasal PHD2 siRNA [90 µg] and administered with AV [130 mg/kg]).

Sensitization, Challenge, and Treatment of Mice

In all models, mice were sensitized on days 0, 7, and 14 with 50 mg Ova (Sigma, Missouri, USA) adsorbed in 4 mg alum or 4 mg alum alone and were challenged from day 21 to 27 with 3% Ova in PBS or PBS alone consecutively, as described earlier. Acute Ova model effect was determined by three independent experiments and both severe model effect was determined by two independent experiments. Dexamethasone (sigma) was dissolved in 50% ethanol and was administered orally (0.75mg/kg) to mice from fourth day of challenge (24th day) till the last day of challenge (27th day), once a day. Similarly, AV (dissolved in distilled water, was given orally (13mg/kg, 65mg/kg, 130mg/kg, 195mg/kg and 260mg/kg and denoted hereafter as AV-D0, AV-D1, AV-D2, AV-D3 and AV-D4, respectively) by gavage from day 24 to 27, once a day. DHB (TCI, Tamilnadu, India) was administered from day 21 to 27 by intraperitoneal injection (10 mg/kg) in 200µl volume of 50% ethanol, was given 2 hours before the Ova challenge. For PHD2 siRNA model, scrambled (Sigma) or PHD2 siRNA (Sigma) was dissolved in ultrapure DNAse and RNAse free water with in vivo-jetPEI as the transfection reagent (Polyplus), was administered intranasally in 90µg concentration to isoflurane-anesthetized mice 2 hours prior to Ova challenge, on day 23, 25 and 27.

Measurement of airway hyperresponsiveness, bronchoalveolar lavage fluid collection, sera separation and histopathology

Airway hyperresponsiveness (AHR) in response to methacholine (Mch, Sigma) was determined in pentobarbital anesthetized mice using flexivent system (Scireq, Canada), as described previously. The results were expressed in the fold change of airway resistance with increasing concentrations of Mch, considering the PBS aerosol induced airway resistance as baseline values. After the AHR measurement, bronchoalveolar lavage fluid (BAL) was collected by instilling 1 ml PBS into the tracheotomised airway and recovered BAL fluids were processed to get cell pellet that will be stained with Leishman stain to determine differential cell count as well as total cell count, as described previously. Blood was withdrawn by cardiac puncture, and serum was separated by centrifugation at 1500 ×g for 10 min and was kept at −70 °C till the measurements of IgE. Lungs were removed and fixed with 10% formalin (3, 4). Fixed lungs were further processed and embedded with paraffin. 5-mm paraffin embedded lung sections then stained with haematoxylin and eosin, periodic acid-Schiff, and Masson Trichrome staining to assess the lung inflammation, mucus hypersecretion and sub-epithelial fibrosis, respectively. Microphotographs were taken by Nikon microscope with camera (Model YS-100). The inflammation scoring was performed as per inflammation grade system by experimentally blind experts to find out the perivascular (PV), peribronchial (PB) lung inflammation to calculate the lung inflammation score (3, 5, 6).

Measurement of Interleukin IL-4, IL-5, IL-13, IL-17, TGF-β1, IFN-γ, PHD2 and HIF-1α

Lung tissue homogenates were used for sandwich ELISA. IL-4, IL-5, TGF-β1, IFN-γ (BD Biosciences), IL-13 (R &D), Il-17 (ebioscience), PHD2 and HIF-1α (USCN), were measured as per manufacturer's instructions and results were expressed in picograms.

Western Blotting

For western blot lung tissue lysate was used. Proteins was separated on 8-10 % sodium dodecyl sulphate-polyacrylamide gel electrophoresis (SDS-PAGE), transferred onto polyvinylidene fluoride (PVDF) membranes (Millipore Corp, USA). Transferred membrane were blocked with blocking buffer (5% or 10% bovine serum albumin "BSA" in phosphate buffered saline with tween 20) or with non-animal protein blocker (NAP, G biosciences). Incubated with primary antibody (abcam, USA or ebiotech, USA) in 1:1000 dilution, followed by HRP conjugated secondary antibody and detected with DAB-H_2O_2 (Sigma, USA) or by chemiluminescence (ECL) method. α-tubulin (Sigma, St. Louis, MO, USA) or β-actin was used as a loading control. Signals were detected by spot densitometry (Image J software).

Transfection, Immunofluorescence and imaging

Human bronchial epithelial cells (BEAS2B) were seeded on glass bottomed dish in 6-well plate and cultured in bronchial epithelial cell growth medium. Cells were transfected with GFP-Mito(mito-GFP) was purchased from addagene as per manufactures instruction. This was generous gift from Dr. Shital (CSIR-IGIB, Delhi). Similarly for immunofluorescence, after appropriate induction, cells

were fixed with 2% paraformaldehyde and permeabilized with 0.1% Triton-X100 (Sigma). Blocking was done with 1.5% BSA. These cells then were labeled with TOM 20 primary antibody (Santacruz), followed by Alexa Fluor 488 (Invitrogen) conjugated secondary antibodies. DAPI (Invitrogen) was used for nuclear staining.

The fluorescent images were collected using point scanning laser confocal microscope system (Nikon A1R-HD, Japan; Leica TCS SP8, Germany) with 60X, 1.4N oil immersion objective lens. The imaging software NIS element AR 5.11.01 and LAX3.1.5 was used to process the raw recorded image data. Modified version of the mitochondrial morphology plugin of ImageJ was used for automated mitochondrial morphometric analysis (7–9).

***In Vitro* Culture of Human Bronchial and Alveolar Epithelial cells**

Human bronchial epithelial cells (BEAS 2B) and adenocarcinomic human alveolar basal epithelial cell line (A549) was obtained from ATCC and cultured in DMEM high glucose medium (obtained from Sigma). For the induction of cellular hypoxia stress cells were treated with DMOG (1 mM/ml, Dimethyloxallyl Glycine, Cayman, 71210) or vehicle (DMSO and distill water) as control. After 8 hours of DMOG treatment, cells were treated with AV extract (10μg/ml), and Dex (10μM/ml). After 24 hrs o treatment, cells were harvested and the levels of HIF-1α was determined in cell lysates (USCN life Science, China) by western blot.

Seahorse assay experiment

Cells were seeded in a 24-well plate of the seahorse format (sup fig), with a seeding density 40000 and 60000 cells per well per 100 µl media for BEAS-2B and A549 respectively. The wells A1, B4, C3 and D6 served as blank and were left without any cells; only media was added to these wells. After 5 hours, when the cells adhered and almost attained morphology, additional 900µl media was added to each well. For the seahorse experiment, following groups were set up: Vehicle (DMSO and distil water), DMOG alone , a DMOG (1mM; 8 hours), AV extract (24 hours), DMOG+Dex (10μM/ml of Dex was added to cells after 8 hours of DMOG treatment and incubated for further 24 hours), DMOG + AV extract (AV extract is added to cells after 8 hours of DMOG treatment and incubated for further 24 hours), and DMOG+Dex+AV. The next day, in fresh media, 1mM DMOG and corresponding volume of DMSO was added to the designated wells. After 8 hours, AV extract (10μg/ml) was added to the respective wells. After 24 hours of AV extract induction, seahorse experiment was initiated to test mitochondrial function and it was determined by XF Cell Mito Stress Test assay using manufacturer's instructions. A day prior to the seahorse experiment, a sensor cartridge was hydrated in Seahorse XF Calibrant at 37°C in a non-CO_2 incubator overnight. On the day of the experiment, assay medium was prepared by adding 1mM pyruvate, 2mM glutamine and 10mM glucose to the basal medium. The pH of the medium was adjusted using 0.1N NaOH and warmed to 37°C until use. After the 24 hours incubation of cells with AV extract, the cell culture media was replaced with the prepared assay medium for 1 hour. After this, the wells were washed thrice with the assay medium. Meanwhile, antibiotics were prepared and added to respective ports

in a constant volume mode. Following were the final concentrations at which the inhibitors was used: Oligomycin 1µM, FCCP 2µM, Rotenone 0.5 µM. Once the plate containing cells is ready and the ports have been loaded with the inhibitors, it was placed in the seahorse instrument and run. After the run, the data was normalised with protein content in each well and analysed further on.

Statistical analysis

All data represents mean ± SEM; n= 3-7 each group; *p <0.05, **p <0.01, ***p <0.001. p-value > 0.05 is considered non-significant (NS). Statistical significance of the differences between paired groups was determined with a two-tailed Student's t test. One-way or two way analysis of variance was used to compare multiple groups and was evaluated further with a nonparametric Mann-Whitney rank-sum test or Kruskal - wallis test wherever appropriate.

Fig. S1. Non-linear effect (U shape curve effect) of AV on physiological parameters of acute asthma. **(A)** LC-MS analysis of aqueous extract of *Adhatoda Vasica* using (+)-ESI-MS for identification of Quinazoline alkaloids. **(B and F)** AV shows U shape curve effect on increased airway resistance in Ova allergic mice in dose dependent manner from D0 to D4. **(C to E)** Representative photomicrographs of mouse lung tissues stained with (C) H&E (4X magnification), (D) PAS (10X magnification), and (E) MT (10X magnification) staining respectively. Black arrow indicates positive staining in respect to particular stain. (**G)** Quantification of peribronchial and perivascular inflammation of lung tissues stained with H&E in using inflammation grade scoring system. **(H and I)** Densitometric analysis of mouse lung tissues stained with PAS and MT to measure mucus metaplasia and collagen deposition respectively using ImageJ. (**J)** Eosinophil abundance in mouse BAL fluid. (**K)** ELISA analysis for TGF-β1 levels in mice lung homogenate. Data are shown as mean ±SEM of three to seven mice per group and representative from at least two independent experiments. Significance denoted by *$P \leq 0.05$, **$P \leq 0.01$, ***$P \leq 0.001$ and ****$P \leq 0.000$; by two way ANOVA (B) and ordinary one way ANOVA (G to K). **Ova-** chicken egg albumin, **Sham**- vehicle (PBS), **Dex**- Dexamethasone (0.75mg/kg), **AV-***Adhatoda Vasica* extract, **D0**- AV 0.130mg/kg, **D1**- AV 65mg/kg, **D2**- AV 130 mg/kg, **D3**- AV 195 mg/kg and **D4**- AV 260mg/kg.

Figure S2: AV restores the HIF-1α induced increased airway inflammation in mitochondria dependent manner. (A) ELISA analysis for HIF-1α levels in mice lung tissue homogenate (n = 3 to 7). **(B)** Representative western blot for HIF-1α abundance in lung tissue lysate of Ova allergic mice treated with Dex or AV in dose dependent manner. **(C)** Correlation analysis of airway

peribronchial inflammation with HIF-1α levels in mice lung after AV-D0, D2, and D4 treatment. **(D)** qPCR for *PHD2* mRNA levels in mice lung RNA samples. Data are shown as mean ±SEM (A to D). **(E)** Western blot for HIF-1α abundance in BEAS2B cell lysate. **(F to I)** Morphological analysis of mitochondria of BEAS2B cells transfected with mitochondria targeted-GFP (mito-GFP) for assessment of mitochondrial network (F), mean branch length (G), area (H), its individual number (I). Data are shown as mean ±SEM of thirty or more cells per group and representative of two independent experiments (E to I). Significance denoted by *$P \leq 0.05$, **$P \leq 0.01$, and ***$P \leq 0.001$; by ordinary one way ANOVA (A), Unpaired t test with Welch's correction (D), ordinary one way ANOVA with Tukey's multiple correction test (F to I). **Sham**- vehicle (PBS), **Dex**- Dexamethasone (0.75mg/kg), **AV-***Adhatoda Vasica* extract, **AV-D0**- AV 0.130mg/kg, **AV-D1**- AV 65mg/kg, **AV-D2**- AV 130 mg/kg, **AV-D3**- AV 195 mg/kg and **AV-D4**- AV 260mg/kg, **Veh-** Vehicle (sterile distill water +DMSO), **BEAS-2B**- normal human bronchial epithelium cells, **DMOG**- dimethyloxaloylglycine, **DMOG+AV**- DMOG+10µg/ml. of AV, **DMOG+Dex**- DMOG+10nM of Dex, **DMOG+Dex+AV**- DMOG+10nM of Dex+10 µg/ml of AV**, DMOG 8hrs**- DMOG treatment for 8 hours.

Figure S3: AV treatment rescues cellular hypoxia induced mitochondrial dysfunction in adenocarcinomic human alveolar basal epithelial cells. (A) Representative OCR levels linked with Basal respiration, ATP production and at Maximum respiration indicated by fold change value as compare to vehicle (sterile distil water) group in adenocarcinomic human alveolar basal epithelial cells (A549). Significance denoted by $ indicates $P \leq 0.0001$ compared to Veh group and **$P \leq 0.01$ and ****$P \leq 0.0001$ compared DMOG group. **(B)** Representative confocal images of cells labelled with mitochondria specific TOM20 show in green, with nuclear stain (DAPI) in blue. Boxed areas in the image are magnified to show typical changes in mitochondria after each treatment and condition. **(C to F)** Dot plot showing statistical score of mitochondrial elongation (C), mitochondrial network (D), area (E) and its individual numbers per cell (F). Data are shown as mean ±SEM of thirty or more cells per group. Significance denoted by *$P \leq 0.05$, **$P \leq 0.01$, ***$P \leq 0.001$ and ****$P \leq 0.0001$, by two way ANOVA with Tukey's multiple correction test (A), ordinary one way ANOVA with Tukey's multiple correction test (C to F). **OCR-** oxygen consumption rate, **DMOG**- dimethyloxaloylglycine, **DMOG+AV**- DMOG+10µg/ml. *Adhatoda Vasica* extract, **DMOG+Dex**- DMOG+10nM of Dexamethasone, **DMOG+Dex+AV**-DMOG+10nM of Dexamethasone+10µg/ml. *Adhatoda Vasica* extract, **DMOG 8hrs**- DMOG treatment for 8 hours.

Figure S4: AV resolves the chemically induced severe corticosteroid insensitive airway inflammation. (A) Quantification of Peribronchial and Perivascular inflammation of lung tissues stained with H&E by inflammation scoring grade method. **(B**.) Densitometric analysis of mouse lung tissues stained with PAS to measure goblet hyperplasia in severe asthmatic mice using

ImageJ **(C to E)** ELISA for IL-13, TNF-α and IFN-γ cytokine levels measured in lung tissue lysate of severe asthmatic mice. Data are shown as mean ±SEM of three to five mice per group and representative of two independent experiment.. Significance denoted by *P ≤0.05, **P≤0.01, ***P≤0.001 and ***P≤0.001; by ordinary one way ANOVA. **Ova-** chicken egg albumin, **Sham-** vehicle (PBS), **DHB**- ethyl, 3,4 -dihydroxy benzoic acid (10mg/kg), **Dex-** Dexamethasone (0.75mg/kg), **AV-D2**- *Adhatoda Vasica* extract (130mg/kg).

Figure S5: AV resolves the *PHD2* siRNA induced severe corticosteroid insensitive airway inflammation. (A) Quantification of Peribronchial inflammation of lung tissues stained with H&E by inflammation scoring grade method. **(B)** Densitometric analysis of mouse lung tissues stained with PAS to mucus metaplasia in severe asthmatic mice using ImageJ. **(C to E)** ELISA analysis of IL-13 (C), KC (D) and IL-6 (E) cytokine levels in lung tissue lysate of severe asthmatic mice. **(F)** Representative photomicrographs of mouse lung tissues stained with PAS to check mucin levels. Arrow indicates positive staining for mucin. Data are shown as mean ±SEM of five to eight mice per group and representative of two independent experiments. Significance indicated by *P ≤ 0.05, **P ≤ 0.01, ***P ≤ 0.001 and ***P ≤ 0.001; by ordinary one way ANOVA. **Ova-** chicken egg albumin, **Sham-** vehicle (PBS), **Scrm siRNA-** scrambled siRNA- 90 μg/mice, **PHD2 siRNA-** mouse specific PHD2 siRNA 90μg/mice., **Dex-** Dexamethasone (0.75mg/kg), **AV-D2-***Adhatoda Vasica* extract (130mg/kg)

Table S1- Liquid chromatography–electrospray ionization–mass spectroscopy of AV extract in positive-ion mode. Identification of Quinazoline alkaloids from the water extract of *Adhatoda Vasica,* separated by mobile phase consist of 0.1% formic acid aqueous solution and acetonitrile. The various peaks obtained (fig. S1A) were analyzed at different time intervals under a gradient program using (+)-ESI-MS.

Sr. No.	RT (in min)	Molecular Formula	$[M+H]^+$ *m/z* (calc)	$[M+H]^+$ *m/z* (exp)	Error (Δppm)	Identification
1	2.4	$C_5H_{14}NO^+$	104.1073	104.1073	0	Choline
2	2.9	$C_5H_{11}NO_2$	118.0864	118.0864	0	Betaine
3	8	$C_{11}H_{12}N_2O_2$	205.0972	205.0974	0.98	Vasicinol/ 5-hydroxy vasicine
4	8.2	$C_{12}H_{12}N_2O_3$	233.0921	233.0921	0	Adhavasicinone
5	10	$C_{11}H_{12}N_2O_2$	205.0972	205.0974	0.98	Vasicinol/ 5-hydroxy vasicine
6	10.4	$C_{12}H_{12}N_2O_2$	217.0972	217.0969	-1.38	Linarinic acid
7	10.9	$C_{11}H_{12}N_2O$	189.1022	189.1022	0	Vasicine
8	13.3	$C_{11}H_{10}N_2O_3$	219.0764	219.0766	0.91	Vasicinolone
9	13.7	$C_{12}H_{14}N_2O_2$	219.1128	219.1131	1.37	5-methoxy vasicine
10	15.7	$C_{17}H_{22}N_2O_6$	351.1551	351.1548	-0.85	Vasicine glycoside
11	15.7	$C_{11}H_{10}N_2O_2$	203.0815	203.0812	-1.48	Vasicinone

Table S2- Liquid chromatography–electrospray ionization–mass spectroscopy of AV extract in negative-ion mode. Identification of flavonoids C- and O- glycosides from the water extract of

Adhatoda Vasica, separated by mobile phase consist of 0.1% formic acid aqueous solution and acetonitrile. The various peaks obtained (fig. S1B) were analyzed at different time intervals under a gradient program using (-)-ESI-MS.

Sr. No	RT (minute)	Molecular Formula	$[M-H]^-$ m/z (calc)	$[M-H]^-$ m/z (exp)	Error (Δppm)	Identification
1	14.8, 17.9	$C_{27}H_{30}O_{16}$	609.1461	609.1464	0.49	Luteolin-6,8-di-C-glucoside/ Quercetin-3-O-rutinoside
2	15.3, 15.8	$C_{26}H_{28}O_{15}$	579.1355	579.1354	-0.17	Luteolin-6-C-glucoside-8-C-arabinoside/ Luteolin-6-C-arabinoside 8-C-glucoside
3	15.5, 18.8	$C_{27}H_{30}O_{15}$	593.1512	593.151	-0.34	Kaempferol-3-O-rutinoside/ Apigenin-6,8-di-C-glucoside
4	15.8, 16.2, 16.5, 16.8, 17.3	$C_{26}H_{28}O_{14}$	563.1406	563.1401	-0.89	Apigenin-6-C-glucoside-8-C-arabinoside/ Apigenin-6-C-arabinoside 8-C-glucoside/ Apigenin-6-C-arabinoside 7-O-glucoside
5	16.6	$C_{25}H_{26}O_{14}$	549.125	549.1253	0.55	Luteolin-6,8-di-C-arabinoside
6	16.7	$C_{21}H_{20}O_{11}$	447.0933	447.0928	-1.12	Luteolin-8-C-glucoside/ Luteolin-6-C-glucoside/ Kaempferol-3-O-glucoside
7	16.8, 17.2, 17.5, 18.1, 18.5	$C_{25}H_{26}O_{13}$	533.1301	533.1303	0.38	Apigenin-6,8-di-C-arabinoside
8	18.1, 18.3	$C_{21}H_{20}O_{10}$	431.0984	431.0983	-0.23	Apigenin-6-C-glucoside/ Apigenin-8-C-glucoside
9	18.6, 19.3	$C_{20}H_{18}O_{10}$	417.0827	417.0831	0.96	Luteolin-8-C-arabinoside/ Luteolin-6-C-arabinoside
10	18.7	$C_{21}H_{20}O_{12}$	463.0882	463.0881	-0.22	Quercetin-3-O-glucoside
11	19.7, 20.1	$C_{20}H_{18}O_9$	401.0878	401.0873	-1.25	Apigenin-8-C-arabinoside/ Apigenin-6-C-arabinoside

Table S3.AV attenuates increased Th2 cytokines levels. Levels of IL-4, 5 and 13 levels in lung homogenate measured by ELISA in acute asthmatic mouse. Data are shown as mean, ± SEM. *P ≤0.05, **P≤0.01 and ***P≤0.001 compared Ova mice group (n = 4-7 per group).

MICE GROUP	IL-4 LEVELS	IL-5 LEVELS	IL-13 LEVELS
SHAM	72.75(±13.56)*	115.08(±34.05)*	147.04(±29.73)*
OVA	124.02(±11.45)	220.33(±23.64)	275.89(±31.69)
OVA+DEX	70.04(±9.77)**	108.73(±16.62)**	124.60(±22.12)**
OVA+D0	48.26(±9.74)**	123.15(±24.48)*	114.79(±20.50)**
OVA+D1	43.64(±10.69)**	103.12(±27.12)*	87.37(±18.69)**
OVA+D2	64.65(±3.89)**	102.37(±13.25)**	89.56(±5.98)**
OVA+D3	74.76(±13.19)**	128.54(±14.35)*	104.20(±14.07)**
OVA+D4	63.29(±7.35)**	128.54(±19.09)*	73.93(±21.42)***

References:

1. S. P., *Charaka Samhita: text with english translation* (Chaukambha Orientalia Publisher, 1981).

2. R. Prasher, D. Pandey, S. De, B. Ravishankar, Standardization of Vasa Ghrta and its extract form and their comparative Pharmaco-Clinical study with special reference to Swasa Roga. *Ayu* **6** (1999).

3. T. Ahmad, *et al.*, Hypoxia Response in Asthma. *Am. J. Respir. Cell Mol. Biol.* **47**, 1–10 (2012).

4. T. Ahmad, U. Mabalirajan, B. Ghosh, A. Agrawal, Altered Asymmetric Dimethyl Arginine Metabolism in Allergically Inflamed Mouse Lungs. *Am. J. Respir. Cell Mol. Biol.* **42**, 3–8 (2010).

5. L. Panda, *et al.*, Linoleic acid metabolite leads to steroid resistant asthma features partially through NF-κB. *Sci. Rep.* **7** (2017).

6. U. Mabalirajan, *et al.*, Mitochondrial structural changes and dysfunction are associated with experimental allergic asthma. *J. Immunol.* **181**, 3540–8 (2008).

7. A. J. Valente, L. A. Maddalena, E. L. Robb, F. Moradi, J. A. Stuart, A simple ImageJ macro tool for analyzing mitochondrial network morphology in mammalian cell culture. *Acta Histochem.* **119**, 315–326 (2017).

8. L. Wiemerslage, D. Lee, Quantification of mitochondrial morphology in neurites of dopaminergic neurons using multiple parameters. *J. Neurosci. Methods* **262**, 56–65 (2016).

9. E. F. Iannetti, J. A. M. Smeitink, J. Beyrath, P. H. G. M. Willems, W. J. H. Koopman, Multiplexed high-content analysis of mitochondrial morphofunction using live-cell microscopy. *Nat. Protoc.* **11**, 1693–1710 (2016).